

Measurement of the integrated luminosities of the data taken by BESIII at $\sqrt{s}=3.650$ and 3.773 GeV*

M. Ablikim(麦迪娜)¹ M. N. Achasov^{8,a} O. Albayrak⁴ D. J. Ambrose⁴¹ F. F. An(安芬芬)¹ Q. An(安琪)⁴²
 J. Z. Bai(白景芝)¹ R. Baldini Ferroli^{19A} Y. Ban(班勇)²⁸ J. Becker³ J. V. Bennett¹⁸ M. Bertani^{19A}
 J. M. Bian(边渐鸣)⁴⁰ E. Boger^{21,b} O. Bondarenko²² I. Boyko²¹ S. Braun³⁷ R. A. Briere⁴ V. Bytnev²¹
 H. Cai(蔡浩)⁴⁶ X. Cai(蔡啸)¹ O. Cakir^{36A} A. Calcaterra^{19A} G. F. Cao(曹国富)¹ S. A. Cetin^{36B}
 J. F. Chang(常劲帆)¹ G. Chelkov^{21,b} G. Chen(陈刚)¹ H. S. Chen(陈和生)¹ J. C. Chen(陈江川)¹
 M. L. Chen(陈玛丽)¹ S. J. Chen(陈申见)²⁶ X. R. Chen(陈旭荣)²³ Y. B. Chen(陈元柏)¹ H. P. Cheng(程和平)¹⁶
 Y. P. Chu(初元萍)¹ D. Cronin-Hennessy⁴⁰ H. L. Dai(代洪亮)¹ J. P. Dai(代建平)¹ D. Dedovich²¹
 Z. Y. Deng(邓子艳)¹ A. Denig²⁰ I. Denysenko²¹ M. Destefanis^{45A,45C} W. M. Ding(丁伟民)³⁰
 Y. Ding(丁勇)²⁴ L. Y. Dong(董燎原)¹ M. Y. Dong(董明义)¹ S. X. Du(杜书先)⁴⁸ J. Fang(方建)¹
 S. S. Fang(房双世)¹ L. Fava^{45B,45C} C. Q. Feng(封常青)⁴² P. Friedel³ C. D. Fu(傅成栋)¹ J. L. Fu(傅金林)²⁶
 O. Fuks^{21,b} Y. Gao(高原宁)³⁵ C. Geng(耿聪)⁴² K. Goetzen⁹ W. X. Gong(龚文煊)¹ W. Gradl²⁰
 M. Greco^{45A,45C} M. H. Gu(顾旻皓)¹ Y. T. Gu(顾运厅)¹¹ Y. H. Guan(管颖慧)³⁸ A. Q. Guo(郭爱强)²⁷
 L. B. Guo(郭立波)²⁵ T. Guo(郭瞰)²⁵ Y. P. Guo(郭玉萍)²⁷ Y. L. Han(韩艳良)¹ F. A. Harris³⁹
 K. L. He(何康林)¹ M. He(何苗)¹ Z. Y. He(何振亚)²⁷ T. Held³ Y. K. Heng(衡月昆)¹ Z. L. Hou(侯治龙)¹
 C. Hu(胡琛)²⁵ H. M. Hu(胡海明)¹ J. F. Hu(胡继峰)³⁷ T. Hu(胡涛)¹ G. M. Huang(黄光明)⁵
 G. S. Huang(黄光顺)⁴² J. S. Huang(黄金书)¹⁴ L. Huang(黄亮)¹ X. T. Huang(黄性涛)³⁰ Y. Huang(黄勇)²⁶
 T. Hussain⁴⁴ C. S. Ji(姬长胜)⁴² Q. Ji(纪全)¹ Q. P. Ji(姬清平)²⁷ X. B. Ji(季晓斌)¹ X. L. Ji(季筱璐)¹
 L. L. Jiang(姜丽丽)¹ X. S. Jiang(江晓山)¹ J. B. Jiao(焦健斌)³⁰ Z. Jiao(焦铮)¹⁶ D. P. Jin(金大鹏)¹
 S. Jin(金山)¹ F. F. Jing(景繁凡)³⁵ N. Kalantar-Nayestanaki²² M. Kavatsyuk²² B. Kloss²⁰ B. Kopf³
 M. Kornicer³⁹ W. Kuehn³⁷ W. Lai(赖蔚)¹ J. S. Lange³⁷ M. Lara¹⁸ P. Larin¹³ M. Leyhe³
 C. H. Li(李春花)¹ Cheng Li(李澄)⁴² Cui Li(李翠)⁴² D. M. Li(李德民)⁴⁸ F. Li(李飞)¹ G. Li(李刚)¹
 H. B. Li(李海波)¹ J. C. Li(李家才)¹ K. Li(李康)¹² Lei Li(李蕾)¹ P. R. Li(李培荣)³⁸ Q. J. Li(李秋菊)¹
 W. D. Li(李卫东)¹ W. G. Li(李卫国)¹ X. L. Li(李晓玲)³⁰ X. N. Li(李小男)¹ X. Q. Li(李学潜)²⁷
 X. R. Li(李秀荣)²⁹ Z. B. Li(李志兵)³⁴ H. Liang(梁昊)⁴² Y. F. Liang(梁勇飞)³² Y. T. Liang(梁羽铁)³⁷
 G. R. Liao(廖广瑞)³⁵ D. X. Lin(Lin)¹³ B. J. Liu(刘北江)¹ C. L. Liu⁴ C. X. Liu(刘春秀)¹
 F. H. Liu(刘福虎)³¹ Fang Liu(刘芳)¹ Feng Liu(刘峰)⁵ H. B. Liu(刘宏邦)¹¹ H. H. Liu(刘汇慧)¹⁵
 H. M. Liu(刘怀民)¹ J. P. Liu(刘觉平)⁴⁶ K. Liu(刘凯)³⁵ K. Y. Liu(刘魁勇)²⁴ P. L. Liu(刘佩莲)³⁰
 Q. Liu(刘倩)³⁸ S. B. Liu(刘树彬)⁴² X. Liu(刘翔)²³ Y. B. Liu(刘玉斌)²⁷ Z. A. Liu(刘振安)¹
 Zhiqiang Liu(刘志强)¹ Zhiqing Liu(刘智青)¹ H. Loehner²² X. C. Lou(娄辛丑)^{1,c} G. R. Lu(鲁公儒)¹⁴
 H. J. Lu(吕海江)¹⁶ J. G. Lu(吕军光)¹ X. R. Lu(吕晓睿)³⁸ Y. P. Lu(卢云鹏)¹ C. L. Luo(罗成林)²⁵
 M. X. Luo(罗民兴)⁴⁷ T. Luo³⁹ X. L. Luo(罗小兰)¹ M. Lv(吕蒙)¹ F. C. Ma(马凤才)²⁴ H. L. Ma(马海龙)¹
 Q. M. Ma(马秋梅)¹ S. Ma(马斯)¹ T. Ma(马天)¹ X. Y. Ma(马骁妍)¹ F. E. Maas¹³ M. Maggiora^{45A,45C}
 Q. A. Malik⁴⁴ Y. J. Mao(冒亚军)²⁸ Z. P. Mao(毛泽普)¹ J. G. Messchendorp²² J. Min(闵建)¹

Received 9 July 2013, Revised 26 August 2013

*Supported by the Ministry of Science and Technology of China (2009CB825204), National Natural Science Foundation of China (10625524, 10821063, 10825524, 10835001, 10935007, 11125525, 11235011), Joint Funds of the National Natural Science Foundation of China (11079008, 11179007), Chinese Academy of Sciences Large-Scale Scientific Facility Program, CAS (KJCX2-YW-N29, KJCX2-YW-N45), 100 Talents Program of CAS, German Research Foundation DFG (Collaborative Research Center CRC-1044), Istituto Nazionale di Fisica Nucleare, Italy, Ministry of Development of Turkey (DPT2006K-120470), U. S. Department of Energy (DE-FG02-04ER41291, DE-FG02-05ER41374, DE-FG02-94ER40823), U.S. National Science Foundation, University of Groningen (RuG) and the Helmholtzzentrum fuer Schwerionenforschung GmbH (GSI), Darmstadt, WCU Program of National Research Foundation of Korea (R32-2008-000-10155-0)

©2013 Chinese Physical Society and the Institute of High Energy Physics of the Chinese Academy of Sciences and the Institute of Modern Physics of the Chinese Academy of Sciences and IOP Publishing Ltd

T. J. Min(闵天觉)¹ R. E. Mitchell¹⁸ X. H. Mo(莫晓虎)¹ H. Moeini²² C. Morales Morales¹³ K. Moriya¹⁸
 N. Yu. Muchnoi^{8,a} H. Muramatsu⁴¹ Y. Nefedov²¹ I. B. Nikolaev^{8,a} Z. Ning(宁哲)¹ S. Nisar⁷
 S. L. Olsen(馬鵬)²⁹ Q. Ouyang(欧阳群)¹ S. Pacetti^{19B} J. W. Park³⁹ M. Pelizaesus³ H. P. Peng(彭海平)⁴²
 K. Peters⁹ J. L. Ping(平加伦)²⁵ R. G. Ping(平荣刚)¹ R. Poling⁴⁰ E. Prencipe²⁰ M. Qi(祁鸣)²⁶
 S. Qian(钱森)¹ C. F. Qiao(乔从丰)³⁸ L. Q. Qin(秦丽清)³⁰ X. S. Qin(秦小帅)¹ Y. Qin(秦瑶)²⁸
 Z. H. Qin(秦中华)¹ J. F. Qiu(邱进发)¹ K. H. Rashid⁴⁴ C. F. Redmer²⁰ G. Rong(荣刚)¹
 X. D. Ruan(阮向东)¹¹ A. Sarantsev^{21,d} M. Shao(邵明)⁴² C. P. Shen(沈成平)² X. Y. Shen(沈肖雁)¹
 H. Y. Sheng(盛华义)¹ M. R. Shepherd¹⁸ W. M. Song(宋维民)¹ X. Y. Song(宋新颖)¹ S. Spataro^{45A,45C}
 B. Spruck³⁷ G. X. Sun(孙功星)¹ J. F. Sun(孙俊峰)¹⁴ S. S. Sun(孙胜森)¹ Y. J. Sun(孙勇杰)⁴²
 Y. Z. Sun(孙永昭)¹ Z. J. Sun(孙志嘉)¹ Z. T. Sun(孙振田)⁴² C. J. Tang(唐昌建)³² X. Tang(唐晓)¹
 I. Tapan^{36C} E. H. Thorndike⁴¹ D. Toth⁴⁰ M. Ullrich³⁷ I. Uman^{36B} G. S. Varner³⁹ B. Wang(王斌)¹
 D. Wang(王东)²⁸ D. Y. Wang(王大勇)²⁸ K. Wang(王科)¹ L. L. Wang(王亮亮)¹ L. S. Wang(王灵淑)¹
 M. Wang(王萌)³⁰ P. Wang(王平)¹ P. L. Wang(王佩良)¹ Q. J. Wang(王庆娟)¹ S. G. Wang(王思广)²⁸
 X. F. Wang(王雄飞)³⁵ X. L. Wang(汪晓莲)⁴² Y. D. Wang(Yadi)^{19A} Y. F. Wang(王贻芳)¹
 Y. Q. Wang(王亚乾)²⁰ Z. Wang(王铮)¹ Z. G. Wang(王志刚)¹ Z. H. Wang(王志宏)⁴² Z. Y. Wang(王至勇)¹
 D. H. Wei(魏代会)¹⁰ J. B. Wei(韦江波)²⁸ P. Weidenkaff²⁰ Q. G. Wen(文群刚)⁴² S. P. Wen(文硕频)¹
 M. Werner³⁷ U. Wiedner³ L. H. Wu(伍灵慧)¹ N. Wu(吴宁)¹ S. X. Wu(吴硕星)⁴² W. Wu(吴蔚)²⁷
 Z. Wu(吴智)¹ L. G. Xia(夏力钢)³⁵ Y. X. Xia(夏宇)¹⁷ Z. J. Xiao(肖振军)²⁵ Y. G. Xie(谢宇广)¹
 Q. L. Xiu(修青磊)¹ G. F. Xu(许国发)¹ Q. J. Xu(徐庆君)¹² Q. N. Xu(徐庆年)³⁸ X. P. Xu(徐新平)³³
 Z. R. Xu(许志蕊)⁴² Z. Xue(薛镇)¹ L. Yan(严亮)⁴² W. B. Yan(鄢文标)⁴² W. C. Yan(闫文成)⁴²
 Y. H. Yan(颜永红)¹⁷ H. X. Yang(杨洪勋)¹ Y. Yang(杨迎)⁵ Y. X. Yang(杨永翔)¹⁰ H. Ye(叶桦)¹
 M. Ye(叶梅)¹ M. H. Ye(叶铭汉)⁶ B. X. Yu(俞伯祥)¹ C. X. Yu(喻纯旭)²⁷ H. W. Yu(于海旺)²⁸
 J. S. Yu(俞洁晟)²³ S. P. Yu(于帅鹏)³⁰ C. Z. Yuan(苑长征)¹ Y. Yuan(袁野)¹ A. A. Zafar⁴⁴ A. Zallo^{19A}
 S. L. Zang(臧石磊)²⁶ Y. Zeng(曾云)¹⁷ B. X. Zhang(张丙新)¹ B. Y. Zhang(张炳云)¹ C. Zhang(张驰)²⁶
 C. C. Zhang(张长春)¹ D. H. Zhang(张达华)¹ H. H. Zhang(张宏浩)³⁴ H. Y. Zhang(章红宇)¹
 J. Q. Zhang(张敬庆)¹ J. W. Zhang(张家文)¹ J. Y. Zhang(张建勇)¹ J. Z. Zhang(张景芝)¹
 LiLi Zhang(张丽丽)¹⁷ S. H. Zhang(张书华)¹ X. J. Zhang(张晓杰)¹ X. Y. Zhang(张学尧)³⁰
 Y. Zhang(张瑶)¹ Y. H. Zhang(张银鸿)¹ Z. P. Zhang(张子平)⁴² Z. Y. Zhang(张振宇)⁴⁶
 Zhenghao Zhang(张正好)⁵ G. Zhao(赵光)¹ J. W. Zhao(赵京伟)¹ Lei Zhao(赵雷)⁴² Ling Zhao(赵玲)¹
 M. G. Zhao(赵明刚)²⁷ Q. Zhao(赵强)¹ S. J. Zhao(赵书俊)⁴⁸ T. C. Zhao(赵天池)¹
 X. H. Zhao(赵祥虎)²⁶ Y. B. Zhao(赵豫斌)¹ Z. G. Zhao(赵政国)⁴² A. Zhemchugov^{21,b} B. Zheng(郑波)⁴³
 J. P. Zheng(郑建平)¹ Y. H. Zheng(郑阳恒)³⁸ B. Zhong(钟彬)²⁵ L. Zhou(周莉)¹ X. Zhou(周详)⁴⁶
 X. K. Zhou(周晓康)³⁸ X. R. Zhou(周小蓉)⁴² K. Zhu(朱凯)¹ K. J. Zhu(朱科军)¹ X. L. Zhu(朱相雷)³⁵
 Y. C. Zhu(朱莹春)⁴² Y. S. Zhu(朱永生)¹ Z. A. Zhu(朱自安)¹ J. Zhuang(庄建)¹
 B. S. Zou(邹冰松)¹ J. H. Zou(邹佳恒)¹

(BESIII collaboration)

¹ Institute of High Energy Physics, Chinese Academy of Sciences, Beijing 100049, China² Beihang University, Beijing 100191, China³ Bochum Ruhr-University, D-44780 Bochum, Germany⁴ Carnegie Mellon University, Pittsburgh, Pennsylvania 15213, USA⁵ Central China Normal University, Wuhan 430079, China⁶ China Center of Advanced Science and Technology, Beijing 100190, China⁷ COMSATS Institute of Information Technology, Lahore, Defence Road, Off Raiwind Road, 54000 Lahore, Pakistan⁸ G. I. Budker Institute of Nuclear Physics SB RAS (BINP), Novosibirsk 630090, Russia⁹ GSI Helmholtzcentre for Heavy Ion Research GmbH, D-64291 Darmstadt, Germany¹⁰ Guangxi Normal University, Guilin 541004, China¹¹ GuangXi University, Nanning 530004, China¹² Hangzhou Normal University, Hangzhou 310036, China¹³ Helmholtz Institute Mainz, Johann-Joachim-Becher-Weg 45, D-55099 Mainz, Germany¹⁴ Henan Normal University, Xinxiang 453007, China

- ¹⁵ Henan University of Science and Technology, Luoyang 471003, China
¹⁶ Huangshan College, Huangshan 245000, China
¹⁷ Hunan University, Changsha 410082, China
¹⁸ Indiana University, Bloomington, Indiana 47405, USA
¹⁹ (A)INFN Laboratori Nazionali di Frascati, I-00044, Frascati, Italy; (B)INFN and University of Perugia, I-06100, Perugia, Italy
²⁰ Johannes Gutenberg University of Mainz, Johann-Joachim-Becher-Weg 45, D-55099 Mainz, Germany
²¹ Joint Institute for Nuclear Research, 141980 Dubna, Moscow region, Russia
²² KVI, University of Groningen, NL-9747 AA Groningen, The Netherlands
²³ Lanzhou University, Lanzhou 730000, China
²⁴ Liaoning University, Shenyang 110036, China
²⁵ Nanjing Normal University, Nanjing 210023, China
²⁶ Nanjing University, Nanjing 210093, China
²⁷ Nankai university, Tianjin 300071, China
²⁸ Peking University, Beijing 100871, China
²⁹ Seoul National University, Seoul, 151-747 Korea
³⁰ Shandong University, Jinan 250100, China
³¹ Shanxi University, Taiyuan 030006, China
³² Sichuan University, Chengdu 610064, China
³³ Soochow University, Suzhou 215006, China
³⁴ Sun Yat-Sen University, Guangzhou 510275, China
³⁵ Tsinghua University, Beijing 100084, China
³⁶ (A)Ankara University, Dogol Caddesi, 06100 Tandogan, Ankara, Turkey; (B)Dogus University, 34722 Istanbul, Turkey; (C)Uludag University, 16059 Bursa, Turkey
³⁷ Universitaet Giessen, D-35392 Giessen, Germany
³⁸ University of Chinese Academy of Sciences, Beijing 100049, China
³⁹ University of Hawaii, Honolulu, Hawaii 96822, USA
⁴⁰ University of Minnesota, Minneapolis, Minnesota 55455, USA
⁴¹ University of Rochester, Rochester, New York 14627, USA
⁴² University of Science and Technology of China, Hefei 230026, China
⁴³ University of South China, Hengyang 421001, China
⁴⁴ University of the Punjab, Lahore-54590, Pakistan
⁴⁵ (A)University of Turin, I-10125, Turin, Italy; (B)University of Eastern Piedmont, I-15121, Alessandria, Italy; (C)INFN, I-10125, Turin, Italy
⁴⁶ Wuhan University, Wuhan 430072, China
⁴⁷ Zhejiang University, Hangzhou 310027, China
⁴⁸ Zhengzhou University, Zhengzhou 450001, China
^a Also at the Novosibirsk State University, Novosibirsk, 630090, Russia
^b Also at the Moscow Institute of Physics and Technology, Moscow 141700, Russia
^c Also at University of Texas at Dallas, Richardson, Texas 75083, USA
^d Also at the PNPI, Gatchina 188300, Russia

Abstract: Data sets were collected with the BESIII detector at the BEPCII collider at the center-of-mass energy of $\sqrt{s}=3.650$ GeV during May 2009 and at $\sqrt{s}=3.773$ GeV from January 2010 to May 2011. By analyzing the large angle Bhabha scattering events, the integrated luminosities of the two data sets are measured to be $(44.49 \pm 0.02 \pm 0.44)$ pb⁻¹ and $(2916.94 \pm 0.18 \pm 29.17)$ pb⁻¹, respectively, where the first error is statistical and the second error is systematic.

Key words: Bhabha scattering events, integrated luminosity, cross section

PACS: 11.30.Rd, 13.66.Bc **DOI:** 10.1088/1674-1137/37/12/123001

1 Introduction

In e^+e^- collider experiments, the number of events for $e^+e^- \rightarrow X$ observed in a data set can be written as

$$N_{e^+e^- \rightarrow X}^{\text{obs}}(\sqrt{s}) = L(\sqrt{s}) \times \epsilon_{e^+e^- \rightarrow X}(\sqrt{s}) \times \sigma^{\text{obs}}(\sqrt{s}), \quad (1)$$

where X denotes some final state produced in e^+e^- annihilation, $N_{e^+e^- \rightarrow X}^{\text{obs}}$ is the number of events observed, $\epsilon_{e^+e^- \rightarrow X}$ is the detection efficiency for $e^+e^- \rightarrow X$, L is the integrated luminosity and $\sigma^{\text{obs}}(\sqrt{s})$ is the observed production cross section for the process $e^+e^- \rightarrow X$ at center-of-mass energy \sqrt{s} .

To systematically study the properties of the production and decays of $\psi(3770)$ and D mesons, a data set was taken at $\sqrt{s}=3.773$ GeV, with the BESIII detector at the BEPCII, from January 2010 to May 2011. So far, this data set is the world's largest e^+e^- collision data set taken around the $\psi(3770)$ resonance peak. In order to estimate the continuum contribution in studies of the resonance decays, another data set was taken in 2009 at $\sqrt{s}=3.650$ GeV, which is far away from the resonance peak. The data taken at $\sqrt{s}=3.773$ GeV was accumulated in different periods of BESIII running; the first part was taken from January 2010 to June 2010 and the

second part was taken from December 2010 to May 2011. For convenience in the following, we call the data taken at $\sqrt{s}=3.650$ GeV the continuum data, and call the two parts of the data taken at $\sqrt{s}=3.773$ GeV $\psi(3770)$ data A and $\psi(3770)$ data B, respectively.

In this paper, we present the measurements of the integrated luminosities of the data sets taken at $\sqrt{s}=3.650$ and 3.773 GeV by analyzing the large angle Bhabha scattering events.

2 BESIII detector

The BESIII detector and the BEPC II collider [1] are major upgrades of the BES II detector and the BEPC collider [2]. The designed peak luminosity of the doubling e^+e^- collider, BEPC II, is 10^{33} $\text{cm}^{-2}\cdot\text{s}^{-1}$ at a beam current of 0.93 A. The peak luminosity at $\sqrt{s}=3.773$ GeV reached 0.65×10^{33} $\text{cm}^{-2}\cdot\text{s}^{-1}$ in April 2011 during the $\psi(3770)$ data taking. The BESIII detector, which has a geometrical acceptance of 93% of 4π , consists of the following main components: 1) a small-celled, helium-based main draft chamber (MDC) with 43 layers. The average single wire resolution is 135 μm , and the momentum resolution for 1 GeV/c charged particles in a 1 T magnetic field is 0.5%; 2) an electromagnetic calorimeter (EMC) made of 6240 CsI(Tl) crystals arranged in a cylindrical shape (barrel) plus two endcaps. For 1.0 GeV photons, the energy resolution is 2.5% in the barrel and 5% in the endcaps, and the position resolution is 6 mm in the barrel and 9 mm in the endcaps; 3) a Time-Of-Flight system (TOF) for particle identification composed of a barrel and two endcaps. The barrel part is made of two layers, each layer consisting of 88 pieces of 5 cm thick, 2.4 m long plastic scintillator. Each endcap consists of 96 fan-shaped, 5 cm thick, plastic scintillators. The time resolution is 80 ps in the barrel, and 110 ps in the endcaps, corresponding to a $2\sigma K/\pi$ separation for momenta up to about 1.0 GeV/c; 4) a muon chamber system (MUC) made of 1600 m^2 of Resistive Plate Chambers (RPC) arranged in 9 layers in the barrel and 8 layers in the endcaps and incorporated in the return yoke of the superconducting magnet. The position resolution is about 2 cm.

3 Method

In principle, any QED process can be used to measure the integrated luminosity of the data set using

$$L(\sqrt{s}) = \frac{N_{\text{QED}}^{\text{obs}}(\sqrt{s}) \times (1-\eta)}{\sigma_{\text{QED}}(\sqrt{s}) \times \epsilon \times \epsilon_{e^+e^-}^{\text{trig}}}, \quad (2)$$

where $N_{\text{QED}}^{\text{obs}}$ is the observed number of events of the final state in question, σ_{QED} is the production cross section, which can be determined by theoretical calculation, ϵ is the detection efficiency, η is the contamination ratio and

$\epsilon_{e^+e^-}^{\text{trig}}$ is the trigger efficiency for collecting the QED process in the on-line data acquisition.

Usually, the processes $e^+e^- \rightarrow (\gamma)e^+e^-$, $e^+e^- \rightarrow (\gamma)\gamma\gamma$ and $e^+e^- \rightarrow (\gamma)\mu^+\mu^-$ are used to measure the integrated luminosity of the data because of their simpler final state topologies, larger production cross sections, higher detection efficiencies, as well as more precise expected cross sections available from theory. In this work, the large angle Bhabha scattering events of $e^+e^- \rightarrow (\gamma)e^+e^-$ are adopted. Throughout the paper, the symbol of “ (γ) ” denotes the possible photon (s) produced due to Initial State Radiation or Final State Radiation.

4 Luminosity measurement

4.1 Event selection

In order to select candidate Bhabha events, it is required that there should be only two good charged tracks, with total charge zero, which are reconstructed in the MDC. Each track must originate from the interaction region $R_{xy} < 1$ cm and $|V_z| < 5$ cm, where R_{xy} and $|V_z|$ are the points of closest approach relative to the collision point in the xy -plane and in the z direction, respectively. Furthermore, to ensure that the candidate charged track hits the barrel of the EMC, we require that the polar angle θ of the charged track satisfies $|\cos\theta| < 0.80$.

Figure 1 shows the energy deposited in the EMC (E_{EMC}) for the good charged tracks of events satisfying the above selection criteria, where the dots with red error bars are the continuum data, the yellow histogram is $e^+e^- \rightarrow (\gamma)e^+e^-$ Monte Carlo events and the light green histogram is $e^+e^- \rightarrow (\gamma)\mu^+\mu^-$ Monte Carlo events. From the figure it can be seen that the requirement

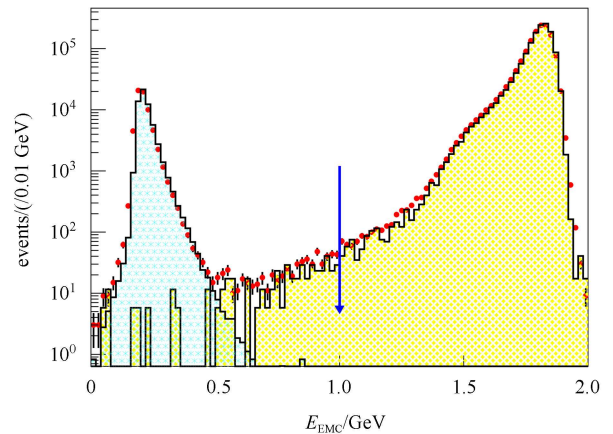


Fig. 1. The distributions of the energy deposited in the EMC from the charged tracks associated with the selected events. The dots with red error bars are the continuum data, the yellow histogram is $e^+e^- \rightarrow (\gamma)e^+e^-$ Monte Carlo events and the light green histogram is $e^+e^- \rightarrow (\gamma)\mu^+\mu^-$ Monte Carlo events.

$E_{\text{EMC}} > 1.0$ GeV can cleanly separate the $e^+e^- \rightarrow (\gamma)\mu^+\mu^-$ events from the Bhabha scattering events. To further remove background from cosmic rays, the momentum of at least one of the two charged tracks in the candidate Bhabha events should be less than $E_b + 0.15$ GeV, where E_b is the calibrated beam energy.

After applying the above selection criteria, the accepted events are mostly Bhabha scattering events. But there may still be a small amount of background from $e^+e^- \rightarrow (\gamma)J/\psi$, $e^+e^- \rightarrow (\gamma)\psi(3686) \rightarrow (\gamma)J/\psi X$ and $e^+e^- \rightarrow \psi(3770) \rightarrow (\gamma)J/\psi X$ ($J/\psi \rightarrow e^+e^-$ and $X = \pi^0\pi^0$, η , π^0 or $\gamma\gamma$). In order to remove these background events, the sum of the momenta of the two good charged tracks is required to be greater than $0.9 \times E_{\text{cm}}$. The remaining contamination from these background sources is estimated by Monte Carlo simulation, which will be discussed in Section 4.3.

4.2 Data analysis

The two oppositely charged tracks in the candidate Bhabha scattering events are bent in the magnetic field, so the positions of their two shower clusters in the xy -plane of the EMC are not back-to-back. To determine the observed number of Bhabha scattering events, we use the difference of the azimuthal angles of the two clusters in the EMC, which is defined as $\delta\phi = |\phi_1 - \phi_2| - 180^\circ$ in degrees, where ϕ_1 and ϕ_2 are the azimuthal angles of the two clusters in the EMC. Fig. 2 shows the $\delta\phi$ distribution of the candidate Bhabha scattering events selected from the continuum data.

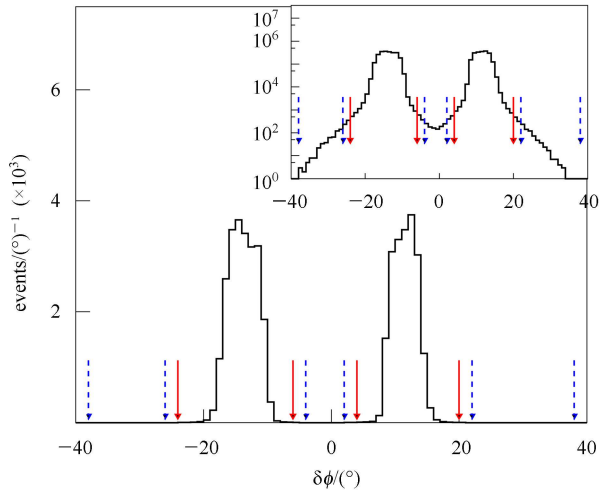


Fig. 2. The distribution of $\delta\phi$ ($\delta\phi = |\phi_1 - \phi_2| - 180^\circ$) for the selected e^+ and e^- tracks. The main part and the inset are shown with linear and logarithmic scale, respectively.

In the figure, the events in the “signal” regions between the red arrows are taken as the signal events, while the ones in the “sideband” regions between the

blue arrows are used to estimate the background in the $\delta\phi$ “signal” region. After subtracting the scaled number of the events in the sideband region from the number of events in the signal region, we obtain the numbers of the Bhabha scattering events observed from data, which are listed in the second row of Table 1.

4.3 Background estimation

For the accepted Bhabha scattering events, there may still be some residual background from $e^+e^- \rightarrow (\gamma)J/\psi$, $e^+e^- \rightarrow (\gamma)\psi(3686) \rightarrow (\gamma)J/\psi X$ and $e^+e^- \rightarrow \psi(3770) \rightarrow (\gamma)J/\psi X$ ($J/\psi \rightarrow e^+e^-$ and $X = \pi^0\pi^0$, η , π^0 or $\gamma\gamma$), as well as some other hadronic decay processes. These are estimated by analyzing the Monte Carlo events, including 16.5 M $e^+e^- \rightarrow (\gamma)J/\psi$, 51 M $e^+e^- \rightarrow (\gamma)\psi(3686)$, 198 M $e^+e^- \rightarrow \psi(3770) \rightarrow D\bar{D}$, 15 M $e^+e^- \rightarrow \psi(3770) \rightarrow \text{non-}D\bar{D}$, and 183 M $e^+e^- \rightarrow \text{continuum light hadron events}$. Detailed analysis gives the contamination rates to be $\eta = 1.7 \times 10^{-5}$ and 1.7×10^{-4} for the candidate Bhabha scattering events selected from the continuum data and the $\psi(3770)$ data, respectively.

4.4 Detection efficiency for $e^+e^- \rightarrow (\gamma)e^+e^-$

To determine the detection efficiencies for the Bhabha scattering events, we generated 400000 $e^+e^- \rightarrow (\gamma)e^+e^-$ Monte Carlo events with the Babayaga generator [3], within the polar angle range of $|\cos\theta| < 0.83$ at $\sqrt{s} = 3.650$ and 3.773 GeV, where θ is the polar angle for the e^+ and e^- . By analyzing these Monte Carlo events with the same selection criteria as the data analysis, we obtained the detection efficiencies for $e^+e^- \rightarrow (\gamma)e^+e^-$ at $\sqrt{s} = 3.650$ and 3.773 GeV, which are summarized in the fourth row of Table 1.

4.5 Integrated luminosities

Inserting the numbers of observed Bhabha scattering events, the detection efficiencies for $e^+e^- \rightarrow (\gamma)e^+e^-$ obtained by the Monte Carlo simulation, the trigger efficiency and the visible cross sections within the polar angle range of $|\cos\theta| < 0.83$ in Eq. (2), we determine the integrated luminosities of the continuum data, the $\psi(3770)$ data A and the $\psi(3770)$ data B to be $(44.49 \pm 0.02 \pm 0.44)$ pb^{-1} , $(927.67 \pm 0.10 \pm 9.28)$ pb^{-1} and $(1989.27 \pm 0.15 \pm 19.89)$ pb^{-1} , respectively, where the first errors are statistical and the second are systematic and discussed in the next section. The total luminosity of the $\psi(3770)$ data is $(2916.94 \pm 0.18 \pm 29.17)$ pb^{-1} . Here, systematic uncertainties are completely correlated between the two parts of the data, and thus are added linearly when they are combined. Here, for the data sets used in the analysis, the trigger efficiency for collecting $e^+e^- \rightarrow (\gamma)e^+e^-$ events was determined to be $\epsilon_{e^+e^-}^{\text{trig}} = 100\%$ with the statistical error being less than 0.1% [4]. The numbers used in the luminosity measurements are summarized in Table 1.

Table 1. Summary of the numbers used in the determination of the luminosities, where $N_{e^+e^- \rightarrow (\gamma)e^+e^-}^{\text{obs}}$ is the number of candidate Bhabha scattering events selected from the data, ϵ is the detection efficiency, σ is the visible cross section for the Bhabha scattering events and L represents the integrated luminosity.

samples	$\psi(3770)$ data A	$\psi(3770)$ data B	continuum data
$N_{e^+e^- \rightarrow (\gamma)e^+e^-}^{\text{obs}} (\times 10^4)$	8412.9±0.9	18140.3±1.3	432.0±0.2
$\eta (\times 10^{-4})$	1.7	1.7	0.17
ϵ (%)	61.28	61.62	61.47
σ/nb	147.9599	147.9599	157.9393
L/pb^{-1}	927.67±0.10±9.28	1989.27±0.15±19.89	44.49±0.02±0.44

4.6 Systematic error

In the measurements of the integrated luminosities, the systematic errors arise from the uncertainties associated with the Bhabha event selection, the Monte Carlo statistics, the background estimation, the signal region selection, the trigger efficiency and the generator.

In order to estimate the systematic uncertainty due to the $\cos\theta$ requirement, we also determine the integrated luminosities with the selection requirements of $|\cos\theta| < 0.75$ and 0.70 . The differences from the standard selection of $|\cos\theta| < 0.80$ are all less than 0.5% for both the continuum data and $\psi(3770)$ data. To be conservative, we take 0.75% as the systematic error due to the $\cos\theta$ selection in this work. The systematic uncertainty due to the MDC measurement information, which includes the uncertainties due to the MDC tracking efficiency and the momentum requirement, is determined to be 0.3% by comparing the integrated luminosities measured with and without the MDC measurement information. The systematic uncertainty due to the E_{EMC} energy selection requirements is determined to be 0.2%, by comparing the E_{EMC} distributions of the data and Monte Carlo events. The uncertainty from the EMC cluster reconstruction is determined to be 0.03% by comparing the efficiencies of the data and the Monte Carlo events.

The uncertainty from the Monte Carlo statistics is 0.1%. The uncertainty in the background subtraction is negligible. The uncertainty due to the $\delta\phi$ signal region selection is estimated to be 0.01% by comparing the integrated luminosities measured with different signal regions. In these measurements, we use the trigger efficiency for collecting $e^+e^- \rightarrow (\gamma)e^+e^-$ events of $\epsilon_{e^+e^-}^{\text{trig}} = 100\%$ with the statistical error being less than 0.1% [4]. Therefore, we take 0.1% as the systematic uncertainty due to trigger efficiency. The uncertainty due

to the Bhabha generator is 0.5%, which is cited from Ref. [3].

Table 2 summarizes the above systematic uncertainties in the luminosity measurement. The total systematic error is determined to be 1.0% by adding these uncertainties in quadrature.

Table 2. The relative systematic uncertainties in the luminosity measurement.

sources	Δ^{sys} (%)
$ \cos\theta < 0.80$	0.75
$E_{\text{EMC}}^+ > 1 \text{ GeV}$	0.2
$E_{\text{EMC}}^- > 1 \text{ GeV}$	0.2
MDC information	0.3
EMC cluster reconstruction	0.03
Monte Carlo statistics	0.1
background estimation	0.0
signal region selection ($\delta\phi$)	0.01
trigger efficiency [4]	0.1
generator [3]	0.5
total	1.0

5 Summary

By analyzing the Bhabha scattering events, we measure the integrated luminosities of the data taken with the BESIII detector at $\sqrt{s} = 3.650$ and 3.773 GeV to be $(44.49 \pm 0.02 \pm 0.44) \text{ pb}^{-1}$ and $(2916.94 \pm 0.18 \pm 29.17) \text{ pb}^{-1}$, respectively. These luminosities can be used for normalization in studies of $\psi(3770)$ production and decays, as well as in studies of D meson production and decays.

The BESIII collaboration thanks the staff of BEPCII and the computing center for their strong support.

References

- 1 Ablikim M et al. (BESIII collaboration). Nucl. Instrum. Methods A, 2004, **614**: 345
- 2 BAI J Z et al. (BESIII collaboration). Nucl. Instrum. Methods A, 1994, **344**: 319; 2001, **458**: 627
- 3 Calame C M C, Montagna G, Nicosini O, Piccinini F. Nucl. Phys. Proc. Suppl., 2004, **131**: 48–55
- 4 Berger N, ZHU Kai et al. Chinese Physics C (HEP & NP), 2010, **34**(12): 1779–1784